sustainability

MDPI

Article

Linking Platform-Recorded Tourism-Resource Supply and Platform-Observed Visitor Interest with Tourist-Flow Networks for Sustainable Tourism Planning: Evidence from the Upper Yangtze River Basin

Yanfeng Wang [1,2,3], Yangjie Li [1], Ying Liu [3,*] and Yishan Zhou [4]

[1] Zhongke-Chongqing Research Institute of Big Data Technology and Application, Chongqing 401331, China; yfwang@cqupt.edu.cn (Y.W.); yangjie19880701@126.com (Y.L.)
[2] School of Communication and Information Engineering, Chongqing University of Posts and Telecommunications, Chongqing 400065, China
[3] The Three Gorges Institute of Ecological Environment, Chongqing Institute of Green and Intelligent Technology, Chinese Academy of Sciences, Chongqing 400714, China
[4] Doctoral School, Polytechnic University of Valencia, 46022 Valencia, Spain; zys_sicau@163.com
* Correspondence: liuying@cigit.ac.cn

Abstract

Sustainable tourism planning in large river basins requires evidence on whether tourism-resource provision, observed visitation, and cross-regional movement coincide. From a recorded-resource–reported-flow–visitor-interest perspective, this study links supply–interest matching with tourist-flow networks in the Upper Yangtze River Basin using Amap point-of-interest datasets and Ctrip and Mafengwo travelogues grouped into three publication-year cohorts (2023–2025). Platform-recorded tourism-resource supply and platform-observed visitor interest were estimated using kernel density estimation with a 30 km search radius and aligned to a 5 km × 5 km grid. Nine matching types were identified using side-specific thresholds fitted to the pooled 2023–2025 distributions and held fixed across cohorts, and reported consecutive visits were reconstructed as directed weighted networks. Recreation represented 43% of recorded supply but 72.39–75.54% of node visits, indicating stronger functional concentration in platform-observed visitor interest. Low-low cells dominated the grid (73.67–75.81%); medium-medium and high-high cells together occupied 5.22–6.14%. Distinguishing these classes shows that the 79.77–81.02% categorical balance primarily reflects low-intensity correspondence. Recorded resource locations formed a core centred on Chengdu–Chongqing and the Sichuan Basin, whereas visitor interest was multicentric and the strongest network nodes clustered in northwestern Yunnan. Within-province transitions dominated; interprovincial transitions represented 11.54–16.56% of total transition weight, with Sichuan–Yunnan and Sichuan–Chongqing forming the main cross-boundary backbone. The combined analysis identifies where recorded resources, visitor interest and itinerary connections converge, informing the selection of areas for visitor monitoring and resource assessment.

Keywords: tourism resources; relative supply–interest matching; tourist-flow network; recorded resource–reported flow–visitor interest; online travelogues; Upper Yangtze River

Check for updates

Academic Editor: Seul Ki Lee

Received: 23 September 2026
Revised: 26 October 2026
Accepted: 28 October 2026
Published: 30 October 2026

Copyright: © 2026 by the authors. Licensee MDPI, Basel, Switzerland. This article is an open access article distributed under the terms and conditions of the Creative Commons Attribution (CC BY) license.

1. Introduction

The United Nations' 2030 Agenda for Sustainable Development explicitly incorporates sustainable tourism into Sustainable Development Goal 12, Responsible Consumption

and Production. Target 12.b specifically calls for the development and implementation of tools to monitor sustainable development impacts associated with tourism [1]. This commitment underscores the urgent need for robust spatial evidence to guide sustainability-oriented tourism planning and management. The location and distribution of tourism resources underpin tourism-product organization, visitor choice, and destination spatial structure [2–6]. Tourism-resource provision, visitor demand, and connectivity among destinations represent distinct dimensions of tourism's spatial organization. Understanding how these dimensions correspond or diverge is therefore essential for improving resource allocation, coordinating tourist movements, and supporting more sustainable destination planning. The analysis contributes to SDG 12.b by identifying locations for independent impact monitoring, providing spatial guidance for subsequent assessment of sustainable-development impacts.

Digital footprints, including points of interest (POIs), online text, geotagged photographs, and trajectories, have broadened the evidence base for tourism planning by revealing where resources are located, which places are visited, and how visits are sequenced [7–9]. Platform-based observations can capture spatial patterns that are difficult to reconstruct from aggregate statistics alone, including visitor concentrations and movements across destinations [10,11]. For travelogue text, sequence analysis captures recorded itinerary order rather than continuously observed mobility [12]. Network studies have further identified core nodes, hierarchical structures, and interregional routes within tourism systems [13,14]. However, platform coverage, user composition, reporting practices, and database updates affect which places and movements are observed, limiting direct inference to the wider tourist population [15–18]. Moreover, digital footprints are often used to describe either spatial concentrations or network structures, leaving the relationship between local resource-visitation patterns and wider tourist movements insufficiently resolved. Digital footprints therefore provide a valuable empirical basis for sustainability-oriented tourism planning, but require an analytical framework that distinguishes local spatial correspondence from connectivity between destinations.

At the local scale, supply–demand matching provides one way to interpret this digital evidence. Existing studies commonly compare the spatial provision of tourism resources or recreational opportunities with observed or estimated demand using kernel density estimation, coupling-coordination models, or categorical combinations [19–21]. Related research on cultural ecosystem services maps capacity, flow, and demand to support landscape and recreation planning [22–24]. Applied studies have also used these relationships to identify spatial synergy, potentially underused resources, and areas of concentrated demand [25,26]. These approaches clarify where resource provision and visitation coincide or diverge, but their planning meaning depends on the level at which correspondence occurs. A low-supply–low-demand area and a high-supply–high-demand area may both be classified as balanced, although they imply substantially different management conditions. In addition, grid-based matching remains place-based: it cannot show whether locally matched areas are connected through reported visit sequences or whether a small number of nodes organize movements across the wider region. Local matching is therefore necessary for diagnosing spatial correspondence, but insufficient for understanding the relational organization of tourism activity.

China's large domestic tourism market has made the spatial organization of tourism resources and visitor movements an increasingly important planning issue. In 2025, Chinese residents made 6.522 billion domestic trips and spent CNY 6.30 trillion on domestic travel [27,28]. National planning documents accordingly emphasize cross-regional tourism-resource integration and a spatial structure characterized by nodal radiation, corridor linkage, and network coordination. They also require resource allocation in the Yangtze

River basin to follow the principles of ecological priority and green development [29,30]. The Upper Yangtze River basin brings these planning concerns together: it extends across multiple provincial jurisdictions and encompasses metropolitan destinations, basin cities, mountain and plateau attractions, and ecologically important areas. Its broad spatial extent, environmental heterogeneity, and cross-administrative structure make it a suitable setting for examining how tourism-resource provision, observed visitation demand, and interregional tourist flows correspond or diverge across space. However, basin-scale evidence integrating these three dimensions remains limited.

Accordingly, this study addresses three interrelated research questions: (1) How do the spatial distributions and concentrations of platform-recorded tourism resources and platform-observed visitor interest differ across the Upper Yangtze River Basin? (2) How are resource supply and visitor interest spatially matched or mismatched, and how do these patterns vary across the 2023–2025 publication-year cohorts under consistent classification criteria? (3) How are reported tourist movements organized into destination networks, and what additional insights does network connectivity provide beyond local supply–interest matching? To structure the empirical analysis, three descriptive propositions are examined: H1, recreation accounts for a greater proportion of recorded node visits than of registered tourism-resource POIs; H2, low-low correspondence constitutes the dominant category among equally classified supply–interest cells; and H3, within-province movements account for the majority of recorded transition weights across all three cohorts. Together, these questions and propositions guide an integrated examination of resource distribution, spatial correspondence, and tourism connectivity. Section 2 describes the analytical framework, data, and methods; Sections 3–5 present the results, discussion, and conclusions.

2. Materials and Methods

2.1. Theoretical Basis and Research Framework

2.1.1. Theoretical Basis

Attraction-system and destination-planning perspectives distinguish the presence of resources from the organization of visitor experiences and connections between places [2–4]. Cultural ecosystem-service frameworks further distinguish potential capacity, realized use and demand [20–24]. These perspectives support examining local resource-interest correspondence and reported inter-attraction connections as different analytical dimensions. We operationalize these dimensions through registered POI density and travelogue occurrences, with indicator definitions given in Section 2.1.3.

In sustainable tourism, greater visitation or closer numerical correspondence must be evaluated against ecological limits and community outcomes. Research on translating recreational ecosystem-service assessment into governance highlights the need to connect spatial diagnosis with decision contexts [25]. This perspective links the spatial analysis to the selection of locations for impact monitoring and capacity assessment.

2.1.2. Literature Synthesis and Analytical Gap

Existing work addresses complementary questions: POI studies describe resource distributions [5,6]; ecosystem-service assessments compare capacity, use and demand [20–24]; spatial-synergy research examines the relation between resources and tourism facilities [26]; and network analyses examine destination connectivity [13,14,31–33]. Recent studies examine tourism infrastructure and recreational-service supply–demand mismatches [34,35], interprovincial and inter-city tourism connections [36,37], and movement patterns derived from GPS and other behavioural data [38,39]. These approaches draw on facility inventories, volunteered records and tracked movement.

This study integrates local supply–interest correspondence and reported itinerary connectivity within a basin-wide framework. The matching analysis identifies where recorded resources and visitor interest coincide or diverge, while the network analysis shows how reported itineraries connect these locations. Their combination shows how local concentrations relate to wider itinerary connections.

2.1.3. Operational Research Framework

Figure 1 presents the research framework, which comprises data preprocessing, three analytical dimensions, and integrated interpretation. Amap tourism-resource POIs and Ctrip and Mafengwo travelogues were first processed through coordinate harmonization, basin clipping, duplicate removal, and POI matching. Tourism-resource POIs represented platform-recorded tourism-resource supply, while travelogue-derived POI occurrences represented platform-observed visitor interest. Their kernel densities were estimated using a common 30 km bandwidth and aligned to a fixed 5 km × 5 km grid to identify nine relative supply–interest combinations. Meanwhile, consecutive POI visits were used to construct a directed weighted tourist-flow network and examine core nodes, route intensity, and regional connections. Finally, the matching and network results were jointly interpreted to distinguish local supply–interest correspondence from cross-node connectivity and to inform differentiated resource allocation, cross-regional route coordination, and sustainable tourism planning.

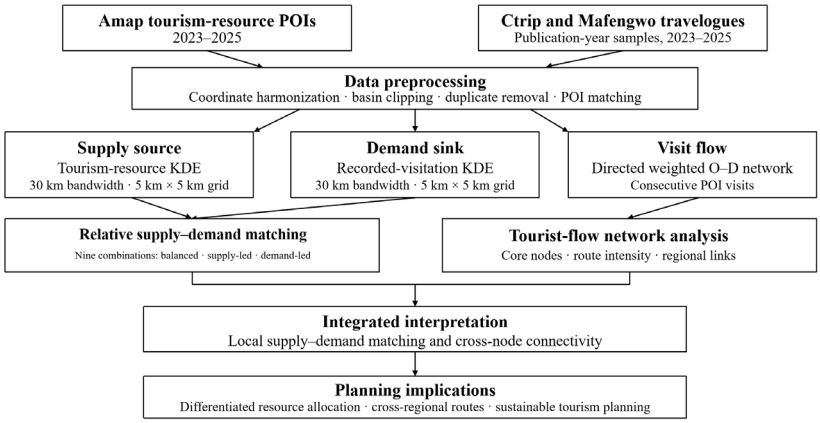

Figure 1. Research framework. In Figure 1, supply and demand denote platform-recorded tourism-resource supply and platform-observed visitor interest, respectively. The arrows connect the data-processing, spatial-classification and network-analysis stages.

Platform-recorded tourism-resource supply refers to the presence and spatial concentration of tourism-resource POIs registered in Amap. Platform-observed visitor interest refers to POI occurrences extracted from Ctrip and Mafengwo travelogues. The two indicators describe registered resources and places reported by platform users, respectively. They are used to examine spatial correspondence, with recorded supply and visitor interest used as shortened terms below. POI density measures registered resource presence, while travelogue occurrences measure reported interest among platform users.

2.2. Study Area

The natural geographical boundary of the Upper Yangtze River basin was adopted to define the study area, which covers approximately 985,400 km^2 across parts of Sichuan, Chongqing, Yunnan, Guizhou, Hubei, Gansu, Shaanxi, Qinghai, and Tibet. The basin has a substantial tourism-resource base; in its Sichuan section alone, official data recorded 592 A-rated tourist attractions in 2022, including 10 5A- and 253 4A-rated attractions [40].

However, metropolitan tourism centres such as Chengdu and Chongqing coexist with ecologically sensitive plateau and mountain destinations. Differences in topography, transport accessibility, and administrative jurisdiction may prevent abundant tourism resources from generating corresponding visitation or effective interregional connections. This contrast makes the basin particularly suitable for examining the matching of platform-recorded tourism-resource supply and platform-observed visitor interest, along with tourist-flow networks within the context of sustainable tourism planning [30]. Both platform-recorded tourism-resource supply and visitor-interest data were clipped to the same basin boundary, and a fixed 5 km × 5 km grid comprising 39,415 analytical cells was applied to ensure spatial comparability across data sources (Figure 2).

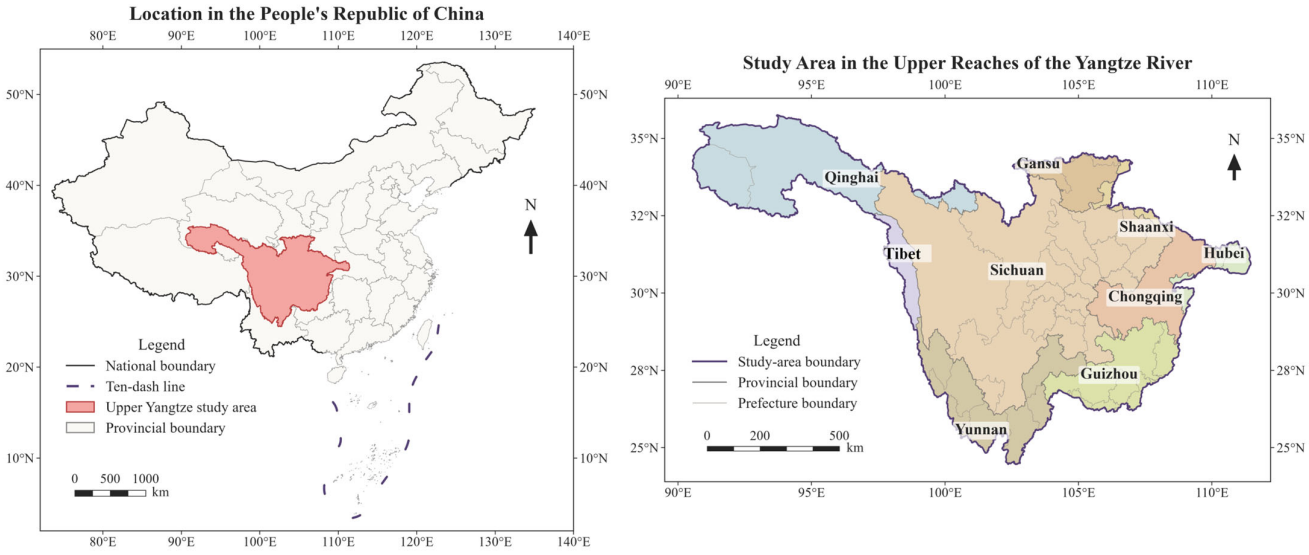

Figure 2. Location and administrative coverage of the study area in the Upper Yangtze River basin.

2.3. Data Sources and Processing

2.3.1. Platform-Recorded Tourism-Resource Supply Data

Tourism-resource POI data for 2023, 2024, and 2025 were obtained from Amap (Figure 3). Following coordinate harmonization, clipping to the study-area boundary, duplicate removal, and attribute standardization, 33,638, 37,843, and 42,047 valid POI records were retained for the three years, respectively. Using a consistent functional classification, the POIs were grouped into four categories: recreation, religious and ritual, public leisure, and scenic and educational resources (Table 1). POI counts were used to describe the number of digitally registered tourism-resource locations, while kernel density represented their spatial concentration. The consistently processed annual datasets thus provided platform-based snapshots for examining the spatial distribution and relative agglomeration of platform-recorded tourism-resource supply. The POI datasets for 2023, 2024 and 2025 were collected independently for each year and checked for duplicate records. The four groups represent broad resource functions for basin-scale comparison. Recreation includes general scenic attractions, religious and ritual resources include places of worship, public leisure includes parks and squares, and scenic and educational resources include observational or educational sites such as zoos and aquaria. Platform type codes, including combined codes, were mapped to one of these four groups for each record.

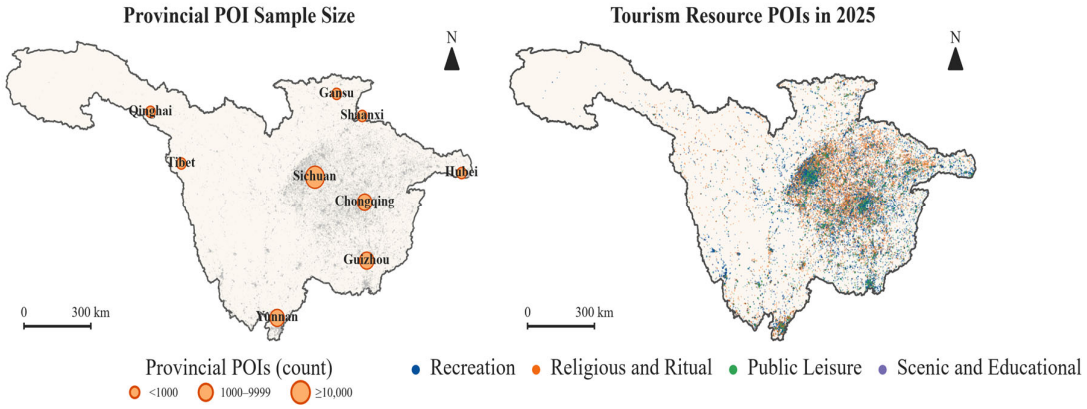

Figure 3. Provincial POI sample size and the spatial distribution of tourism-resource POIs in 2025.

Table 1. Classification and numerical composition of tourism-resource POIs in the Upper Yangtze River, 2023–2025.

Reclassified Category	Representative Amap POI Types	2023 (*n*)	2024 (*n*)	2025, *n* (Share, %)
Recreation	Scenic areas, national and provincial attractions, viewpoints, etc.	14,458	16,266	18,073 (42.98)
Religious and ritual	Buddhist and Daoist temples, churches, mosques, etc.	9672	10,881	12,090 (28.75)
Public leisure	Parks, plazas, civic squares, beaches, etc.	8146	9164	10,182 (24.22)
Scenic and educational	Memorial halls, red-tourism sites, etc.	1362	1532	1702 (4.05)

2.3.2. Platform-Observed Visitor Interest and Route Data

Visitor-interest and route data were extracted from travelogues published on Ctrip and Mafengwo between 2023 and 2025 and organized by publication year. After removing within-platform URL duplicates and exact cross-platform duplicates, attraction names and aliases were matched to the tourism-resource POI gazetteer. POI identities were determined by combining place names, administrative locations, and coordinates. The recognized POIs in each travelogue were arranged according to their reported order. Travelogues containing at least one study-area POI were included in visitor-interest estimation, while adjacent POI pairs in travelogues containing two or more recognized POIs were converted into directed O-D links. Repeated links were aggregated to measure route intensity. The two platform datasets were then merged for each annual cohort, with identical construction rules applied to within-province and interprovincial links. Because publication dates may differ from actual travel dates, the annual cohorts are interpreted as publication-year samples, and the resulting O-D links represent reported consecutive visits. The 2023, 2024, and 2025 cohorts contained 2030, 1854, and 1806 valid travelogues, respectively, yielding 10,001, 10,573, and 10,440 recorded node visits and 2243, 2244, and 2266 unique POI nodes (Table 2).

We compared travelogue activity with Baidu inbound migration indices in selected regional subsets using temporally matched observations. Travelogues were grouped by the source collection-province field (src_prov) and aligned by publication date. Activity was represented by (1) the number of distinct travelogues containing at least one matched POI and (2) the sum of matched POIs across travelogues, counting each POI at most once per travelogue. For each reporting interval, the mean daily inbound migration index was calculated when at least five observed days were available for a week, ten for a fortnight, or

twenty for a month. Spearman rank correlations were used to assess temporal correspondence across weekly, biweekly and monthly aggregation scales where matched observations were available.

Table 2. Processing summary of online travelogue samples, 2023–2025.

Publication Year	Valid Travelogues (n)	Recorded Node Visits (n)	Weighted O-D Transitions (n)	Unique POI Nodes (n)	Directed Edges (n)
2023	2030	10,001	7971	2243	5812
2024	1854	10,573	8719	2244	6159
2025	1806	10,440	8634	2266	6237

Platform participation and reporting choices shape the geography recorded in social media [15–18]. To characterize this variation, we compared category shares across platforms. Recreation accounted for 75.86–80.32% of Ctrip node occurrences and 69.04–72.11% of Mafengwo occurrences, compared with about 43% of POIs. These proportions describe differences in the resource types represented by each platform.

2.4. Methods

2.4.1. Kernel Density Estimation

Kernel density estimation (KDE) quantified the spatial concentration of registered tourism POIs and travelogue-derived POI occurrences within two-dimensional neighbourhoods [5,6,41,42]. For n sample points, with the i-th point located at x_i and bandwidth h, the general two-dimensional KDE is expressed as:

$$f(x) = \frac{1}{nh^2}\sum_{i=1}^{n} K\left(\frac{x - x_i}{h}\right) \quad (1)$$

where $f(x)$ is the estimated kernel density at location x; $K[(x - x_i)/h]$ is the kernel function; n is the number of observations; and $\boldsymbol{h}$ is the bandwidth. Kernel density estimation assigned a unit weight to each POI or recorded occurrence, representing the frequency of records. The analysis used a 30 km bandwidth to represent regional concentrations. Both surfaces were calculated at a 5 km cell size, expressed as density per square kilometre, and projected and aligned to the same fixed grid. These standardized settings provided the basis for identifying relative spatial agglomeration and conducting supply–interest matching within each publication-year cohort.

The 5 km grid provides a common reporting unit for basin-wide comparisons. Each 25 km^2 cell summarizes the surrounding KDE surface: urban cells may combine several attractions, whereas rural cells may contain few recorded points while receiving density contributions from neighbouring locations. Grid size determines the spatial detail represented by the classification and is therefore relevant to the scale component of the modifiable areal unit problem (MAUP).

2.4.2. Spatial Supply–Interest Matching

To assess local relationships between platform-recorded tourism-resource supply and platform-observed visitor interest, we classified the continuous KDE values on the common 5 km grid. The first and 99th percentiles were estimated from pooled 2023–2025 densities separately for supply and visitor interest. Values outside these limits were clipped, and the retained interval was scaled to 0–1 using the same parameters for all three cohorts. This reduces the influence of extreme density peaks while retaining a common cross-year scale. Grid-based comparison provides a consistent spatial unit for identifying the correspondence

and mismatch between recorded supply and visitor interest surfaces [19–21]. For grid cell i, normalized visitor interest X_i and normalized supply Y_i were calculated as:

$$X_i = [\text{clip}(x_i, P1{,}x, P99{,}x) - P1{,}x]/(P99{,}x - P1{,}x) \quad (2)$$

$$Y_i = [\text{clip}(y_i, P1{,}y, P99{,}y) - P1{,}y]/(P99{,}y - P1{,}y) \quad (3)$$

Here, x_i and y_i denote visitor-interest and recorded-supply KDE values. P1,x and P99,x are the first and 99th percentiles of the pooled interest values; P1,y and P99,y are the corresponding supply percentiles. The clip function replaces values below P1 with P1 and values above P99 with P99. Each side contains 118,245 cell-cohort observations, including zero values. Jenks natural breaks were fitted once to each side's transformed pooled distribution and applied unchanged to all cohorts [43]. The raw-density breakpoints are 0.055701 and 0.197304 POIs/km^2 for supply and 0.016708 and 0.057724 node records/km^2 for visitor interest. Low values are at or below the first breakpoint, medium values lie above the first and at or below the second, and high values exceed the second. Combining the two classes in interest-supply order yields nine types. Low-low, medium-medium and high-high are relatively balanced; low-medium, low-high and medium-high are supply-led; medium-low, high-low and high-medium are interest-led. Relative balance denotes equality of indicator classes. The common transformation and thresholds support comparisons across publication-year samples within each indicator.

2.4.3. Tourist-Flow Network Construction and Metrics

Each standardized Amap POI, identified by its name, administrative location, coordinates, and unique Amap identifier, was treated as a network node. Attraction-level POIs and subordinate POIs within larger attractions were retained as separate nodes when they had distinct Amap identifiers. All network metrics are therefore interpreted at POI level. Within each travelogue, consecutive POIs formed directed edges in their reported order, following sequence-based analysis of travel-blog content [12]. Repeated transitions in the same direction were aggregated as edge weights. Let W_{ij} denote the cumulative number of observed transitions from node $\boldsymbol{i}$ to node $\boldsymbol{j}$. The weighted out-strength of node i is:

$$S_i^{\text{out}} = \sum_{j \in N} W_{ij} \quad (4)$$

The total strength of node i combines incoming and outgoing transitions to measure its overall connection intensity:

$$S_i = S_i^{\text{in}} + S_i^{\text{out}} = \sum_{j=1}^{n} \left(W_{ij} + W_{ji} \right) \quad (5)$$

where S_i^{in} and S_i^{out} denote the weighted in-strength and out-strength of node i, respectively. Total strength S_i was used to rank core POIs because it represents the total volume of weighted connections associated with each node [44–46]. Directionality was retained to represent the reported O-D order and to identify reciprocal and interprovincial connections. Network structure was characterized by the number of nodes, number of unique directed edges, total edge weight, network density, mean edge weight, share of reciprocal directed edges, maximum node strength, and the volume and share of interprovincial transitions. These indicators were interpreted jointly to describe network scale, connection intensity, reciprocity, and cross-regional connectivity. For each publication-year cohort, Ctrip and Mafengwo records were combined using the same network-construction rules, with both within-province and interprovincial O-D links retained. This consistent specification supported the identification of core POIs, major travel routes, and differences in network organization among the three cohorts. We assessed sampling uncertainty in

the interprovincial share by resampling whole travelogues within each cohort, retaining their transitions together and including travelogues with no transitions. We generated 5000 replicates and calculated percentile 95% intervals. A further comparison resampled 1806 travelogues from the 2023 cohort to assess the effect of sample size.

2.4.4. Software and Reproducibility

Spatial data preprocessing, coordinate transformation, kernel density estimation, grid alignment, and cartographic visualization were performed using ArcMap 10.8 (Esri Inc., Redlands, CA, USA). Data compilation and descriptive statistics were conducted using Microsoft Excel 2019 (Microsoft Corporation, Redmond, WA, USA). All spatial datasets were processed using a WGS 84-based Lambert azimuthal equal-area projection centred at 101° E and 30° N, with zero false easting and northing and linear units in metres. The computational workflow used annual point records and a fixed 5 km × 5 km grid. All surfaces were aligned to the same fixed grid before supply–interest matching. Tourist-flow networks were constructed from standardized O-D tables derived from consecutive POI visits, and the network metrics were calculated according to the definitions provided in Section 2.4.3. Consistent spatial parameters, matching rules, and network definitions were applied to all publication-year cohorts to support methodological reproducibility and the comparison of relative spatial structures. P1-P99 scaling, exact Fisher-Jenks classification and matching maps were implemented in Python 3.12 (Python Software Foundation, Wilmington, DE, USA).

3. Results

3.1. Spatial Pattern of Platform-Recorded Tourism-Resource Supply

3.1.1. Composition of Tourism-Resource Types

Following consistent data processing, the Amap tourism-resource datasets contained 33,638 POIs in 2023, 37,843 in 2024, and 42,047 in 2025. Recreation consistently constituted the largest category, accounting for approximately 43% of the total, followed by religious and ritual resources (28.8%), public leisure resources (24.2%), and scenic and educational resources (4.0%). In 2025, the four categories comprised 18,073, 12,090, 10,182, and 1702 POIs, respectively, corresponding to 42.98%, 28.75%, 24.22%, and 4.05% of the total. Between 2023 and 2025, the number of platform-recorded POIs increased by 8409, including 3615 recreation POIs, 2418 religious and ritual POIs, 2036 public leisure POIs, and 340 scenic and educational POIs (Figure 4). Despite the larger record count in the later dataset, the proportional structure remained largely unchanged. Recreation and religious and ritual resources continued to form the main components of platform-recorded tourism-resource supply, whereas scenic and educational resources accounted for a comparatively small share.

3.1.2. Spatial Agglomeration of Tourism Resources

Across 2023–2025, platform-recorded tourism-resource supply displayed a stable core-periphery pattern (Figure 5). A continuous high-density belt extended across the Chengdu–Chongqing region and the urban areas of the Sichuan Basin, while secondary clusters were distributed around Kunming, Guiyang, Zunyi, northwestern Yunnan, and northwestern Sichuan. Tourism resources in the plateau and mountain areas were more dispersed and generally occurred at lower densities. In 2025, Sichuan contained 22,245 POIs and Chongqing contained 9702, accounting for 52.91% and 23.07% of the study-area total, respectively. Their combined share reached 75.98%. Yunnan and Guizhou contributed a further 10.48% and 9.45%, bringing the combined share of these four provincial-level regions to 95.91%. Overall, the basin was characterized by a dominant Chengdu–Chongqing–Sichuan Basin core and

several secondary regional centres. The persistence of this spatial configuration indicates a stable but uneven distribution of platform-recorded tourism-resource supply, highlighting regional balance and differentiated resource organization as important considerations for sustainable tourism planning at the river-basin scale.

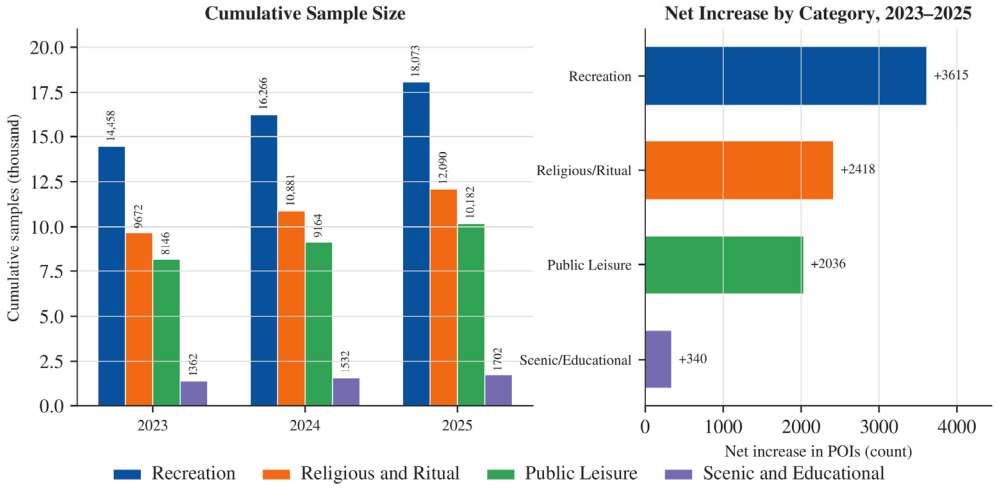

Figure 4. Sample size and category composition of tourism-resource POIs, 2023–2025.

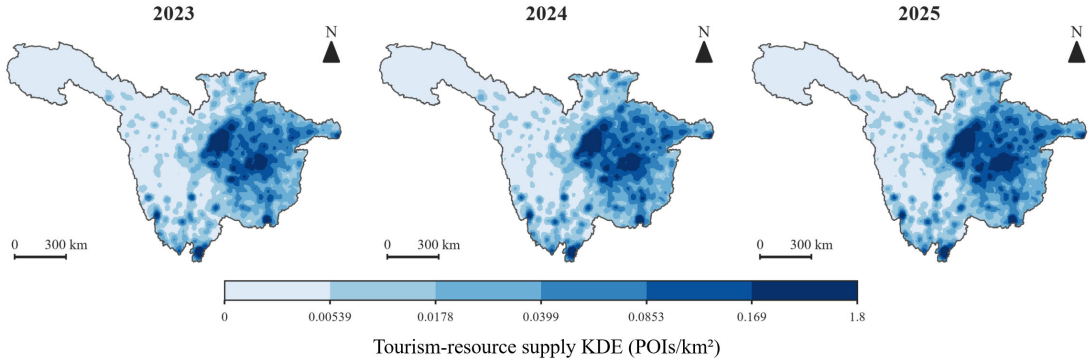

Figure 5. Kernel-density distribution of platform-recorded tourism-resource supply in the Upper Yangtze River basin, 2023–2025. All panels use the same 30 km search radius, 5 km cell size, classification thresholds, and KDE colour scale. Supply denotes the spatial concentration of registered POI locations, not service capacity.

3.2. Spatial Pattern of Platform-Observed Visitor Interest

3.2.1. Composition of Platform-Recorded Visits by Resource Type

Platform-recorded visitation was consistently dominated by recreation resources, which accounted for 74.81%, 75.54%, and 72.39% of recorded node visits in 2023, 2024, and 2025, respectively. Public-leisure and religious and ritual resources formed the second tier, with annual shares of 11.53–13.60% and 11.21–11.87%, respectively, whereas scenic and educational resources remained the least visited category, accounting for only 1.72–2.15% (Table 3). Between 2023 and 2025, the share of recreation visits decreased by 2.42 percentage points, while the share of public-leisure visits increased by 1.60 percentage points. Religious and ritual resources and scenic and educational resources recorded smaller increases of 0.64 and 0.19 percentage points, respectively. Composition was broadly similar across the three samples. Recreation accounted for more than 72% of recorded visits in every cohort, substantially exceeding its approximately 43% share of platform-recorded tourism-resource supply reported in Section 3.1.1. This contrast indicates that platform-observed visitor

interest was more strongly concentrated by resource function than the recorded supply, providing interest-side evidence for assessing functional balance and diversified resource use in sustainable tourism planning.

Table 3. Composition of platform-recorded node visits by tourism-resource type, 2023–2025 (%).

Resource Type	2023 (%)	2024 (%)	2025 (%)
Recreation	74.81	75.54	72.39
Religious and ritual	11.23	11.21	11.87
Scenic and educational	1.96	1.72	2.15
Public leisure	12.00	11.53	13.60

3.2.2. Sample Size and Spatial Distribution by Publication Year

The 2023, 2024, and 2025 publication-year cohorts comprised 2030, 1854, and 1806 valid travelogues, respectively. Although the number of valid travelogues decreased across the three cohorts, the corresponding numbers of recorded node visits were 10,001, 10,573, and 10,440, while the numbers of consecutive transitions were 7971, 8719, and 8634 (Table 2). The mean number of recognized nodes per travelogue consequently increased from 4.93 in 2023 to 5.70 in 2024 and 5.78 in 2025, indicating that the later cohorts contained longer recognized visit sequences on average.

Median intervals between reported departure and publication in the Mafengwo records were 24, 25 and 27 days for the three cohorts.

Under a common KDE scale, platform-observed visitor interest exhibited a persistent multicentric spatial pattern across the three publication-year cohorts (Figure 6). The Chengdu–Chongqing region and the urban areas of the Sichuan Basin, together with northwestern Yunnan, formed the principal visitor-interest hotspots throughout the study period. Central Guizhou and central Yunnan also repeatedly formed distinct clusters, while smaller concentrations occurred around attraction clusters in northwestern Sichuan. The 2023 sample showed pronounced concentrations in Chengdu–Chongqing, central Guizhou, and northwestern Yunnan. The 2024 and 2025 samples retained these principal hotspots, with additional secondary concentrations becoming evident in central Yunnan and northwestern Sichuan. Inter-cohort differences were therefore expressed mainly in the intensity and spatial extent of existing clusters rather than in the emergence of an entirely different visitor-interest structure. Overall, platform-observed visitor interest remained concentrated in a limited number of metropolitan and scenic clusters while being distributed across several regional centres. This persistent multicentric pattern provides a spatial basis for evaluating regional balance in visitor distribution and coordinating tourism flows in sustainable tourism planning at the river-basin scale.

We compared travelogue activity with Baidu inbound migration indices in selected regional subsets using temporally matched observations. Spearman rank correlations identified six positive associations ($p < 0.05$). In Tibet in 2024, travelogue counts were positively correlated with the index at weekly ($\rho = 0.413$, $p = 0.0032$), biweekly ($\rho = 0.511$, $p = 0.0107$), and monthly ($\rho = 0.715$, $p = 0.0133$) scales. Weekly POI-record counts also showed a positive correlation ($\rho = 0.312$, $p = 0.0292$). In 2025, positive correlations were observed for biweekly POI-record counts in Guizhou ($\rho = 0.441$, $p = 0.0243$) and biweekly travelogue counts in Sichuan ($\rho = 0.410$, $p = 0.0375$). These results indicate temporal correspondence in the selected regional subsets.

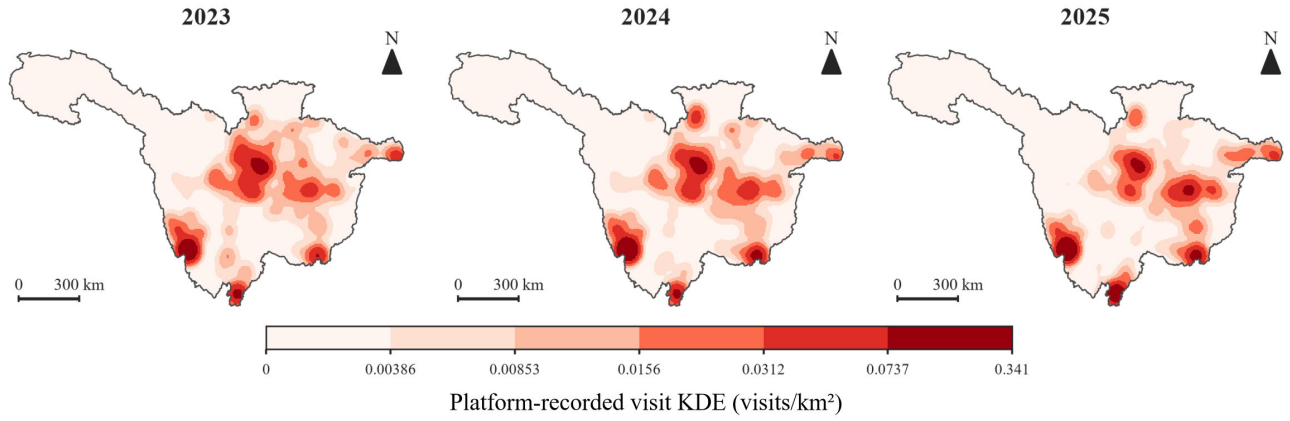

Figure 6. Kernel-density distribution of platform-observed visitor interest by travelogue publication year, 2023–2025. All panels use the same 30 km bandwidth, 5 km cell size, and KDE colour scale. Recorded node occurrences are used as a proxy for visitor interest, not total visitation or demand.

3.3. Spatial Patterns of Matching Between Platform-Recorded Tourism-Resource Supply and Platform-Observed Visitor Interest

Low-low correspondence dominated all three publication-year samples, accounting for 73.67–75.81% of the grid (Figure 7); medium-medium and high-high cells together occupied only 5.22–6.14%. Low-low cells occupied most peripheral parts of the basin, where both platform-recorded tourism-resource supply and platform-observed visitor interest remained at relatively low levels. Medium-medium and high-high cells formed localized matching areas under the fixed thresholds. Supply-led cells were distributed mainly around established resource clusters and their adjacent areas, while interest-led cells were particularly evident in northwestern Yunnan and at several isolated tourism nodes. The locations of the principal matching cores and mismatch areas remained broadly consistent from 2023 to 2025. Overall, the basin combined extensive low-level correspondence with localized high-level matching and supply- or interest-led mismatch. This spatial configuration reveals an uneven relationship between tourism-resource provision and observed visitation, highlighting regional balance and differentiated resource organization as important considerations for sustainable tourism planning at the river-basin scale.

Low-low correspondence predominated across all three cohorts, while localized high-high areas occurred in each year.

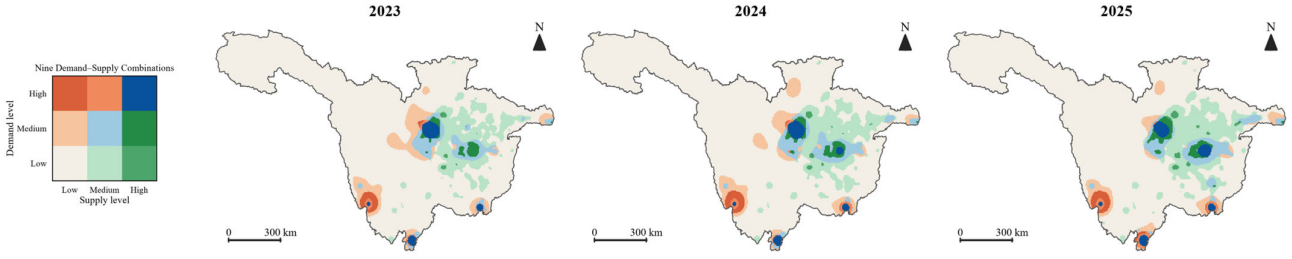

Figure 7. Spatial distribution of relative matching of platform-recorded tourism-resource supply and platform-observed visitor interest types, 2023–2025. In the legend, Supply denotes platform-recorded tourism-resource supply and Demand denotes platform-observed visitor interest; the same shorthand applies in Figures 8–10. P1–P99 scaling and Jenks thresholds are fixed across years, separately for each indicator.

3.3.1. Composition and Spatial Distribution of Relatively Balanced Cells

Low-low cells numbered 29,879, 29,075, 29,039, accounting for 75.81%, 73.77%, 73.67% of the grid in 2023, 2024 and 2025, respectively (Figure 8). Including medium-medium

and high-high cells gives categorical-balance shares of 81.02%, 79.77%, 79.81%. Low-low cells represented 92.31–93.56% of the relatively balanced group. Medium-medium cells accounted for 3.99%, 4.58%, 4.54%, and high-high cells accounted for 1.23%, 1.42%, 1.60%. High-high counts were 483, 561, 632; the 2024 high-high class comprised 561 cells (1.42%). The maps distinguish extensive low-level correspondence from localized medium- and high-level matching areas.

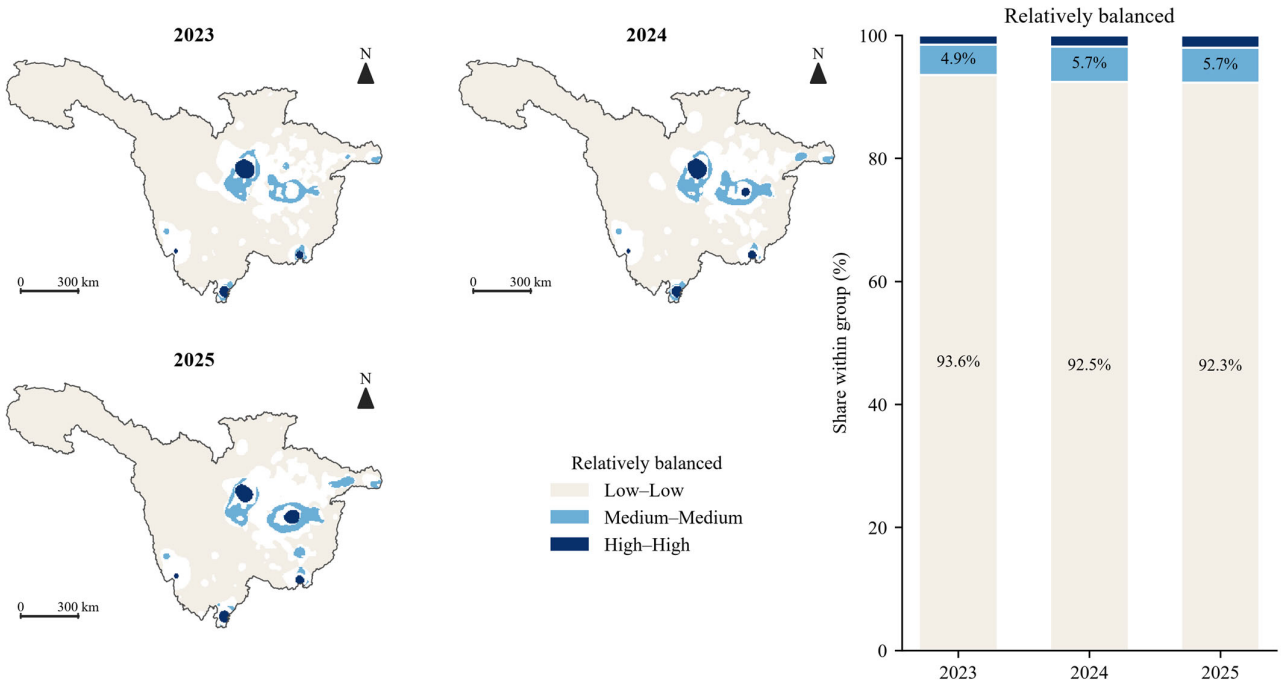

Figure 8. Spatial distribution and within-group composition of relatively balanced supply–interest matching cells, 2023–2025. The stacked bars show the shares of low-low, medium-medium, and high-high cells within the relatively balanced group for each publication-year cohort. Relative balance denotes correspondence between proxy classes, not capacity-demand equilibrium. P1–P99 scaling and Jenks thresholds are fixed across years, separately for each indicator.

3.3.2. Composition and Spatial Distribution of Supply-Led Cells

Supply-led cells, comprising low-medium, low-high and medium-high combinations, accounted for 11.51%, 12.81%, 14.25% of the grid in 2023, 2024 and 2025, respectively (Figure 9). Low-medium was the dominant subtype, with 4037, 4439, 4803 cells. Low-high cells numbered 88, 122, 225, and medium-high cells numbered 411, 490, 587. These areas identify locations where the resource-density class exceeds the visitor-interest class. Their distribution is shown in Figure 9, with most supply-led cells exhibiting a one-level difference.

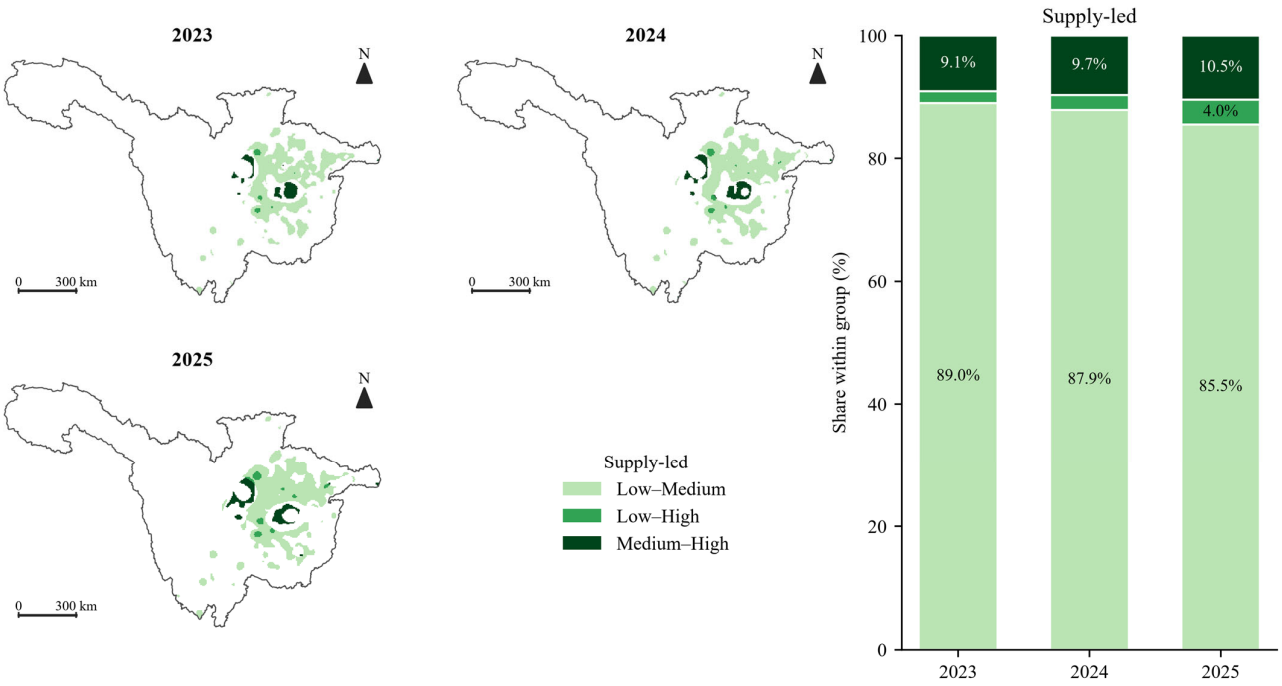

Figure 9. Spatial distribution and within-group composition of supply-led tourism-resource matching cells, 2023–2025. The stacked bars show the shares of low-medium, low-high, and medium-high cells within the supply-led group for each publication-year cohort. Low-high cells occurred in all three cohorts. Supply-led denotes a higher recorded-resource class than the visitor-interest class. P1–P99 scaling and Jenks thresholds are fixed across years, separately for each indicator.

3.3.3. Composition and Spatial Distribution of Interest-Led Cells

Interest-led cells, comprising medium-low, high-low and high-medium combinations, accounted for 7.47%, 7.41%, 5.94% of the grid in 2023, 2024 and 2025, respectively (Table 4; Figure 10). Total counts were 2943, 2922, 2341. Medium-low remained the largest subtype, with 2467, 2319, 1667 cells. High-low cells numbered 328, 390, 411, while high-medium cells numbered 148, 213, 263. The share of high-interest combinations within this group was 16.2%, 20.6%, 28.8%. These areas identify concentrations where the visitor-interest class exceeds the recorded-resource class.

Table 4. Composition of the three major relative supply–interest matching categories by publication-year cohort.

Publication Year	Relatively Balanced (%)	Supply-Led (%)	Interest-Led (%)
2023	81.02	11.51	7.47
2024	79.77	12.81	7.41
2025	79.81	14.25	5.94

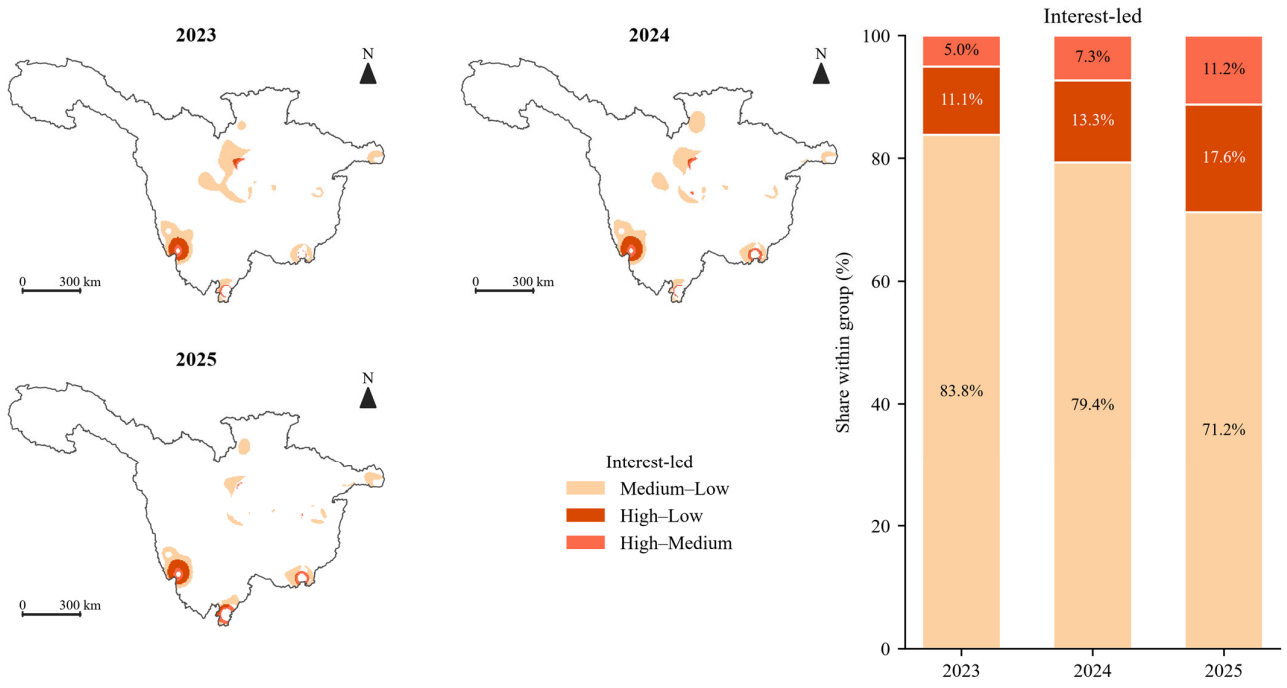

Figure 10. Spatial distribution and within-group composition of interest-led tourism-resource matching cells, 2023–2025. The stacked bars show the shares of medium-low, high-low, and high-medium cells within the interest-led group for each publication-year cohort. Interest-led cells have a higher visitor-interest class than the recorded-supply class. P1–P99 scaling and Jenks thresholds are fixed across years, separately for each indicator.

3.4. Tourist-Flow Network Structure and Connectivity

3.4.1. Overall Network Structure

The three publication-year networks contained 2243, 2244, and 2266 POI nodes in 2023, 2024, and 2025, respectively, indicating broadly stable node coverage (Table 5). The number of directed edges increased from 5812 in 2023 to 6159 in 2024 and 6237 in 2025. Total edge weight increased from 7971 to 8719 between 2023 and 2024 and remained at a similar level in 2025, with a value of 8634. Network density increased slightly from 0.00116 to 0.00122 and then remained stable, while mean edge weight varied within a narrow range of 1.37–1.42. The later cohorts therefore contained a broader set of directed connections, while the average repetition of each connection remained relatively stable. The share of reciprocal directed edges declined from 16.79% to 15.10% and 14.11%, indicating that a smaller proportion of links had a corresponding reverse direction. At the same time, maximum node strength increased from 395 to 584 and 587, showing higher recorded strength of the leading POI in the later samples. The three sample networks shared a sparse structure, with differences in the number and strength of recorded connections. These structural features provide network-based evidence for evaluating route diversification, hub prominence, and the regional distribution of visitor movements in sustainable tourism planning.

Table 5. Structural metrics of platform-observed tourist-flow networks by publication-year cohort, 2023–2025.

Metric	2023	2024	2025
Number of POI nodes	2243	2244	2266
Number of directed edges	5812	6159	6237
Total edge weight	7971	8719	8634

Table 5. *Cont.*

Metric	2023	2024	2025
Network density	0.00116	0.00122	0.00122
Mean edge weight	1.37	1.42	1.38
Share of reciprocal directed edges (%)	16.79	15.10	14.11
Maximum node strength	395	584	587

3.4.2. Core POIs and Node Hierarchy

The hierarchy of core POIs remained stable across the three publication-year networks, with the same three attractions in northwestern Yunnan occupying the highest positions (Figure 11). In 2023, the three strongest nodes were Yulong Snow Mountain National Scenic Area, Lijiang Old Town, and Shuhe Ancient Town, with total node strengths of 395, 339, and 279, respectively. Yulong Snow Mountain remained the strongest node in 2024 and 2025, with its strength increasing to 584 and 587. Shuhe Ancient Town moved to second place in 2024 and retained this position in 2025, with strengths of 509 and 487, while Lijiang Old Town ranked third, with strengths of 405 and 400. A second tier of high-strength nodes included Kuanzhai Alley, Jiayu Pavilion, Ciqikou Ancient Town, Dujiangyan Scenic Area, and Qianling Mountain Park, although their prominence varied among the three cohorts. Overall, the network hierarchy combined a dominant core-node cluster in northwestern Yunnan with a group of urban and attraction nodes elsewhere in the basin.

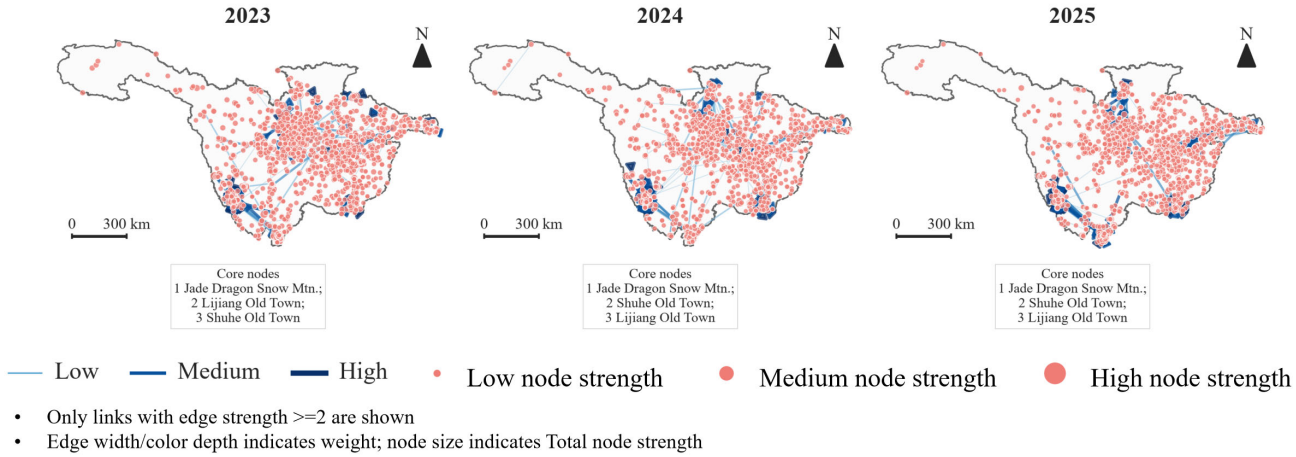

Figure 11. Platform-observed tourist-flow networks in the Upper Yangtze River basin, 2023–2025. Node size represents total node strength, while line width and colour intensity represent edge weight. Nodes with total strength ≥ 5 and links with edge weight ≥ 2 are displayed. Arrowheads indicate the direction of selected high-weight links, and the inset boxes list the three strongest nodes in each publication-year cohort.

3.4.3. Interprovincial Connectivity and the Regional Network Backbone

Within-province transitions remained the dominant component of the tourist-flow networks, numbering 7051, 7468, and 7204 in 2023, 2024, and 2025 and accounting for 88.46%, 85.65%, and 83.44% of total edge weight, respectively. Interprovincial transitions increased from 920 in 2023 to 1251 in 2024 and 1430 in 2025, raising their share from 11.54% to 14.35% and 16.56%. Within-province connections thus dominated each sample. After combining reciprocal directions for each provincial pair, Sichuan–Yunnan and Sichuan–Chongqing were the strongest interprovincial connections in all three cohorts. The weighted connection between Sichuan and Yunnan increased from 290 to 374 and 400, while that between Sichuan and Chongqing increased from 190 to 304 and 376. Sichuan–Guizhou recorded 96, 156,

and 138 weighted transitions, and the Chongqing–Yunnan connection reached 156 in 2025. Together, Sichuan, Chongqing, Yunnan, and Guizhou formed a persistent regional network backbone. The main cross-regional routes connected the high-strength POIs of northwestern Yunnan with major nodes in Chengdu–Chongqing, central Guizhou, and central Yunnan (Figure 11). The 2025 interprovincial share exceeded the 2023 share by 5.02 percentage points; the bootstrap interval for this difference excluded zero.

4. Discussion

4.1. Functional Selectivity and Uneven Spatial Concentration of Platform-Recorded Supply and Platform-Observed Visitor Interest

Recent studies using social-media traces, activity data, and infrastructure indicators have shown that observed tourism demand tends to cluster where recognizable attractions, urban services, and accessibility overlap [34,35,47]. The Upper Yangtze River exhibits the same broad tendency, but at a wider and more heterogeneous scale. Chengdu–Chongqing and the Sichuan Basin formed the main concentration of platform-recorded resources, while platform-observed visitor interest also retained strong centres in northwestern Yunnan, central Yunnan, and central Guizhou. This difference suggests two overlapping geographies: a metropolitan service core and a set of attraction-led destination cores. The distinction is important because the places that organize tourism services are not necessarily the same places that attract the most repeated visits.

Functional composition sharpens this distinction. Recreation represented about 43% of the POI supply but 72.39–75.54% of all recorded node visits. Religious and ritual, public-leisure, and scenic and educational resources were therefore less likely to enter travelogue itineraries relative to their representation in the POI inventory. A plausible mechanism is selective itinerary formation. Recreation-oriented attractions may be easier to combine into itineraries, and platform visibility may contribute to their prominence. This interpretation is consistent with evidence that non-local tourist networks are more polarized around well-known nodes and that infrastructure conditions are associated with observed visitation [34,47].

Compared with studies that map resource supply or visitation hotspots separately, this study compares digitally registered resource locations with POI occurrences in reported itineraries. Its main advance is to show that diversity in the POI inventory does not necessarily correspond to diversity in travelogue-recorded interest. For sustainable tourism, this changes the planning question from where more attractions should be added to which existing cultural, educational, religious, or public-leisure resources can be integrated into viable itineraries without exceeding local ecological and social capacity. Broadening demand across functions could reduce dependence on a narrow set of recreation nodes, but promotion should be selective rather than universal.

4.2. Low-Level Correspondence and the Core-Periphery Logic of Supply–Demand Matching

Low-low cells accounted for 73.67–75.81% of the grid and 92.31–93.56% of the relatively balanced group. The categorical-balance share of 79.77–81.02% therefore mainly reflects low-intensity correspondence. A Tibetan Plateau study using a related classification also identified low-low correspondence as the largest type, with a share of 59.5% [48]. Under pooled P1-P99 scaling, high-high cells occurred in every cohort, including 561 cells in 2024. This distinction separates widespread low-level correspondence from localized high-level matching; the category labels describe the specified density classes.

Two considerations help interpret this pattern. First, medium- and high-level correspondence may reflect the co-location of population, facilities and accessibility around major destinations. Evidence from urban and regional recreation studies likewise links

supply–demand mismatches to distance from urban centres, accessibility, and the spatial concentration of users [35,49]. Second, the POI measure captures named and platform-recorded tourism resources, not the full ecological or cultural potential of a landscape. Studies that treat naturalness and landscape opportunity as potential supply often identify remote natural areas as high-supply/low-demand zones [50]. In this study, many remote plateau and mountain cells instead appear as low-low. The difference reveals a conceptual boundary: potential recreational endowment is not equivalent to digitally registered tourism-resource locations.

Supply-led and interest-led cells clarify the edges of this pattern. Supply-led areas often surrounded established clusters, suggesting that recorded resources had not been incorporated into visits at the same relative intensity. Interest-led cells were fewer and more compact, indicating selective concentration on a limited set of destinations rather than a basin-wide resource deficit. Similar studies have used mismatch maps to design differentiated tourism and landscape interventions [49,51]. The present results add a level-sensitive interpretation: categorical agreement should not be labelled sustainable coordination until its intensity and ecological setting are considered. In low-low areas, low recorded activity may reflect poor connection, conservation priorities, or both. Development decisions therefore require an overlay of ecological sensitivity, protected-area status, community needs, and access conditions.

4.3. From Spatial Matching to Networked Movement: Hub Dominance and Route Hierarchy

Static matching alone cannot explain how destinations function as a regional system. Research on cultural ecosystem services has shown that supply, demand, and service flows can occupy different locations and follow different spatial logics [52]. The Upper Yangtze River results show the same separation at the tourism-resource level. Large low-low areas existed alongside a sparse network organized around a few high-strength nodes. Thus, local equality of supply and demand classes does not imply that a place is integrated into tourist movement, and a strong network position does not require locally extensive resource supply.

Previous tourism network studies report that larger markets can strengthen Matthew effects and core-periphery organization, while rural networks remain low-density and depend strongly on resource quality and transport access [53,54]. The persistent dominance of Yulong Snow Mountain, Shuhe Ancient Town, and Lijiang Old Town accords with this logic. Geographic and thematic proximity may favour their joint inclusion in reported itineraries, where repeated transitions increase node strength. Chengdu–Chongqing played a different role. Studies of the economic circle identify a dual-core flow structure associated with transport, accommodation, and urban service capacity [55]. Taken together, the evidence suggests a division between attraction cores in northwestern Yunnan and metropolitan gateway-like areas in Chengdu–Chongqing. These two forms of centrality can coexist within the same basin network.

In the later publication-year cohorts, the number of directed links was higher, whereas the reciprocal-edge share was lower and maximum node strength was greater. This combination is consistent with broader route coverage that remained concentrated around leading nodes. It does not indicate that the network became more integrated. Itinerary efficiency may help explain these connections, consistent with research on route organization [53,54]. This interpretation points to transport links, visitor information and route coordination as priorities for planning assessment. At the same time, routing more visitors through already dominant hubs can intensify congestion and pressure. Planning assessments should therefore consider visitor dispersal alongside pressure at the connecting nodes.

4.4. Interprovincial Connectivity and the River-Basin Tourism Backbone

The dominance of within-province transitions is consistent with recent evidence that intra-regional or intracoupled tourism remains the main component of interprovincial cultural ecosystem service flows in China [36]. Provincial transport systems, destination marketing and trip-time constraints may contribute to this pattern. Within the publication-year samples, the interprovincial share rose from 11.54% to 16.56%, while Sichuan–Yunnan and Sichuan–Chongqing remained the strongest pairs. The evidence therefore identifies a stable cross-boundary backbone rather than a set of isolated provincial systems.

Studies of the Yangtze River Delta describe tourist flows as polarized radial sub-networks around major cities, whereas GPS-based research in Gansu and Qinghai highlights node-corridor-network organization along long-distance circuits [37,38]. The Upper Yangtze River combines elements of both. Chengdu and Chongqing operate as dense urban gateways, while northwestern Yunnan supplies a high-attraction node cluster connected through a limited number of long-distance axes. Spatial proximity may help explain the strong Sichuan–Chongqing links. Sichuan–Yunnan connections may also benefit from complementary urban, mountain, heritage, and ethnic-tourism products. The main advance over province-bounded studies is to show how administrative organization and basin-scale visitor movement overlap rather than coincide.

For sustainable tourism, stronger interprovincial connectivity is valuable only if it improves coordination and distributes pressure. The principal corridors provide a basis for shared route design, integrated public-transport information, common signage, and coordinated monitoring. Secondary nodes should be added according to access, community benefit, and carrying capacity, not simply because they lie near a major corridor. Joint management is especially important where a popular route links ecologically sensitive mountain destinations with metropolitan gateways. In this setting, the purpose of regional integration is not to maximize flow volume. It is to direct flows toward locations that can accommodate them while protecting places that should remain low-intensity.

4.5. Theoretical Contributions and Practical Implications for Sustainable Tourism

The study makes three theoretical contributions. First, it introduces a level-sensitive reading of supply–interest matching: equal relative classes describe correspondence, but low-low correspondence is not equivalent to high-quality coordination. Second, it links local proxy classes to platform-recorded itinerary sequences. The grid reveals where supply and platform-observed visitor interest coincide; the directed network reveals how those places are organized through consecutive visits. This extends supply–demand-flow research [52] by representing reported attraction-level transitions within a large natural basin. Third, the recorded-resource–reported-flow–visitor-interest perspective treats the basin as a cross-administrative tourism system. It describes how recorded resource concentrations, visitor-interest clusters and reported connecting sequences coexist at different locations.

Integrating spatial matching patterns with tourist-flow networks reveals distinct regional characteristics that can inform differentiated tourism planning across the Upper Yangtze River Basin. In northwestern Yunnan, Yulong Snow Mountain, Lijiang Old Town, and Shuhe Ancient Town consistently ranked as the three strongest network nodes, while surrounding areas exhibited concentrated visitor interest relative to recorded tourism resources. This spatial pattern suggests that tourism management should prioritize assessing visitor concentrations, destination carrying capacity, and opportunities to distribute itineraries toward suitable alternative attractions, rather than further intensifying activity around established hubs. In contrast, the Chengdu–Chongqing region exhibited a high concentration of recorded tourism resources, with supply-led areas distributed around established tourism clusters. These areas offer potential opportunities to improve the utilization of

existing resources through better itinerary connections and regional tourism integration, provided that accessibility, ecological constraints, and local community interests are considered. At the interprovincial scale, the persistent dominance of Sichuan–Yunnan and Sichuan–Chongqing connections highlights the importance of coordinated route planning, tourism information sharing, and cross-boundary visitor management. Meanwhile, the extensive low-low areas should not be interpreted simply as opportunities for tourism expansion, since low recorded activity may reflect limited platform coverage, accessibility constraints, or ecological conservation requirements. Taken together, these findings support a spatially differentiated planning approach that prioritizes managing concentrated visitor interest, improving connections among existing tourism resources, strengthening interprovincial coordination, and protecting ecologically sensitive areas.

Recent sustainable-destination research argues that combining actual movement evidence with visitor experience can support crowd dispersal and a more even spatial distribution of benefits [39]. By integrating spatial matching patterns with reported itinerary networks, this framework provides a more comprehensive understanding of how tourism-resource concentrations, visitor interest, and destination connectivity interact across the Upper Yangtze River Basin. The combined analysis helps distinguish areas characterized by concentrated visitor interest, strong network connectivity, or limited recorded tourism activity, thereby providing a spatial basis for differentiated tourism management. Incorporating protected-area boundaries, ecological conservation redlines, and environmental impact indicators into subsequent assessments would further clarify where tourism concentrations may intersect with ecological constraints and where management interventions should be prioritized. From a basin-wide perspective, sustainable tourism planning should therefore emphasize the complementary roles of different destinations rather than pursuing uniformly higher levels of resource development or visitor activity. Such an approach can support more targeted resource management, visitor dispersal, and ecological protection while recognizing that the underlying mechanisms inferred from the observed spatial associations require further empirical verification.

4.6. Transferability and Platform Dependence

The proposed framework can be extended to other regions where georeferenced tourism-resource inventories and itinerary records containing identifiable destinations and visit sequences are available. Its application requires adapting resource classifications, POI-matching procedures, spatial scales, and classification thresholds to local geographical conditions and data characteristics while maintaining consistent analytical standards for temporal comparisons. Platforms such as Google Maps, TripAdvisor, and Wikiloc may provide complementary data sources, although their suitability depends on geographical coverage, data accessibility, and the availability of reconstructable visit sequences. Where sequential itinerary records are insufficient, additional mobility or itinerary data are needed to support network analysis, while spatial resource-interest matching can still be undertaken independently.

5. Conclusions

This study integrated Amap tourism-resource POIs and Ctrip and Mafengwo travelogues within a common 5 km grid and a directed weighted network to examine platform-recorded tourism-resource supply, platform-observed visitor interest, relative matching, and tourist flows in the Upper Yangtze River from a recorded-resource–reported-flow–visitor-interest perspective. Recorded resources formed a concentrated core, whereas visitor interest was multicentric. Recreation occupied a larger share of node occurrences than of POI records, consistent with H1. Resource supply was relatively diverse, whereas recorded

visits were strongly concentrated in recreation-oriented nodes. Consistent with H2, low-low cells dominated the grid (73.67–75.81%), while medium-medium and high-high cells together accounted for 5.22–6.14%; the larger categorical-balance share of 79.77–81.02% therefore did not represent high-level coordination. At the network scale, high-strength attractions in northwestern Yunnan coexisted with gateway-like concentrations in Chengdu–Chongqing. Within-province transitions dominated all three samples, consistent with H3, while Sichuan–Yunnan and Sichuan–Chongqing formed the main recorded interprovincial backbone. Together, these patterns distinguish the concentration of registered resources from the distribution and connectivity of reported visitor interest. By linking local matching with consecutive inter-node visits, the study shows that digitally registered resource presence, platform-observed visitor interest, and reported network connectivity are related but not interchangeable dimensions of sustainable tourism. This distinction provides a basis for differentiated resource allocation, visitor-pressure management, and cross-provincial route coordination. The framework supports basin-scale planning by identifying resource concentrations, areas of concentrated visitor interest and interprovincial itinerary connections. These locations provide a spatial basis for the tourism-impact monitoring envisaged in SDG 12.b.

The selected regional comparisons with independently sourced Baidu inbound migration indices showed positive temporal associations with travelogue activity. The pooled P1–P99 normalization and fixed Jenks thresholds provide a consistent basis for comparing the basin-wide spatial patterns across the three cohorts. Nevertheless, the analysis primarily identifies spatial patterns and network relationships, while site-specific carrying capacity and ecological impacts require additional assessment. Future research could integrate destination-level visitor statistics, environmental indicators, and protected-area constraints to translate these findings into more precise tourism management strategies. Overall, the proposed framework provides an integrated basis for identifying regional tourism disparities, improving cross-regional coordination, and supporting differentiated sustainable tourism planning.

Author Contributions: Conceptualization, Y.W. and Y.L. (Ying Liu); methodology, Y.W.; software, Y.W.; validation, Y.L. (Yangjie Li) and Y.Z.; formal analysis, Y.W.; investigation, Y.Z.; resources, Y.L. (Yangjie Li); data curation, Y.W.; writing—original draft preparation, Y.W.; writing—review and editing, Y.L. (Ying Liu); visualization, Y.L. (Yangjie Li); supervision, Y.L. (Ying Liu); project administration, Y.W.; funding acquisition, Y.W. All authors have read and agreed to the published version of the manuscript.

Funding: This study was supported by grants from Humanities and Social Sciences Research Project of Chongqing Municipal Education Commission (25SKGH357).

Institutional Review Board Statement: Not applicable.

Informed Consent Statement: Not applicable.

Data Availability Statement: The datasets used and analyzed during the current study are available from the corresponding author on reasonable request.

Conflicts of Interest: The authors declare no conflict of interest.

References

1. United Nations. *Transforming Our World: The 2030 Agenda for Sustainable Development; Resolution A/RES/70/1*; United Nations: New York, NY, USA, 2015. Available online: https://sdgs.un.org/2030agenda (accessed on 21 September 2026).
2. Lew, A.A. A framework of tourist attraction research. *Ann. Tour. Res.* **1987**, *14*, 553–575. [CrossRef]
3. Leiper, N. Tourist attraction systems. *Ann. Tour. Res.* **1990**, *17*, 367–384. [CrossRef]
4. Dredge, D. Destination place planning and design. *Ann. Tour. Res.* **1999**, *26*, 772–791. [CrossRef]

5. Zhang, X.; Han, H.; Tang, Y.; Chen, Z. Spatial distribution characteristics and driving factors of tourism resources in China. *Land* **2023**, *12*, 1029. [CrossRef]
6. Qu, X.; Xu, G.; Qi, J.; Bao, H. Identifying the spatial patterns and influencing factors of leisure and tourism in Xi'an based on point of interest (POI) data. *Land* **2023**, *12*, 1805. [CrossRef]
7. Li, J.; Xu, L.; Tang, L.; Wang, S.; Li, L. Big data in tourism research: A literature review. *Tour. Manag.* **2018**, *68*, 301–323. [CrossRef]
8. Wood, S.A.; Guerry, A.D.; Silver, J.M.; Lacayo, M. Using social media to quantify nature-based tourism and recreation. *Sci. Rep.* **2013**, *3*, 2976. [CrossRef]
9. Vu, H.Q.; Li, G.; Law, R.; Ye, B.H. Exploring the travel behaviors of inbound tourists to Hong Kong using geotagged photos. *Tour. Manag.* **2015**, *46*, 222–232. [CrossRef]
10. Tenkanen, H.; Di Minin, E.; Heikinheimo, V.; Hausmann, A.; Herbst, M.; Kajala, L.; Toivonen, T. Instagram, Flickr, or Twitter: Assessing the usability of social media data for visitor monitoring in protected areas. *Sci. Rep.* **2017**, *7*, 17615. [CrossRef]
11. Mou, N.; Zheng, Y.; Makkonen, T.; Yang, T.; Tang, J.; Song, Y. Tourists' digital footprint: The spatial patterns of tourist flows in Qingdao, China. *Tour. Manag.* **2020**, *81*, 104151. [CrossRef]
12. Yuan, H.; Xu, H.; Qian, Y.; Li, Y. Make your travel smarter: Summarizing urban tourism information from massive blog data. *Int. J. Inf. Manag.* **2016**, *36*, 1306–1319. [CrossRef]
13. Shi, S.; Liu, M.; Xi, J. Hierarchical structure and organizational model of county tourism network of the Tibetan Plateau. *Land* **2022**, *11*, 1880. [CrossRef]
14. Jiang, X.; Song, X.; Zhao, H.; Zhang, H. Rural tourism network evaluation based on resource control ability analysis: A case study of Ning'an, China. *Land* **2021**, *10*, 427. [CrossRef]
15. Toivonen, T.; Heikinheimo, V.; Fink, C.; Hausmann, A.; Hiippala, T.; Järv, O.; Tenkanen, H.; Di Minin, E. Social media data for conservation science: A methodological overview. *Biol. Conserv.* **2019**, *233*, 298–315. [CrossRef]
16. Mancini, F.; Coghill, G.M.; Lusseau, D. Using social media to quantify spatial and temporal dynamics of nature-based recreational activities. *PLoS ONE* **2018**, *13*, e0200565. [CrossRef]
17. Zhang, G.; Zhu, A.-X. The representativeness and spatial bias of volunteered geographic information: A review. *Ann. GIS* **2018**, *24*, 151–162. [CrossRef]
18. Senaratne, H.; Mobasheri, A.; Ali, A.L.; Capineri, C.; Haklay, M. A review of volunteered geographic information quality assessment methods. *Int. J. Geogr. Inf. Sci.* **2017**, *31*, 139–167. [CrossRef]
19. Liu, J.; Ji, X.; Lu, J.; Zhang, T. Research on matching supply and demand of tourism resources in Jiaodong Economic Circle based on multi-source heterogeneous data. *J. Geo-Inf. Sci.* **2024**, *26*, 393–407. (In Chinese)
20. Burkhard, B.; Kroll, F.; Nedkov, S.; Müller, F. Mapping ecosystem service supply, demand and budgets. *Ecol. Indic.* **2012**, *21*, 17–29. [CrossRef]
21. Wolff, S.; Schulp, C.J.E.; Verburg, P.H. Mapping ecosystem services demand: A review of current research and future perspectives. *Ecol. Indic.* **2015**, *55*, 159–171. [CrossRef]
22. Paracchini, M.L.; Zulian, G.; Kopperoinen, L.; Maes, J.; Schägner, J.P.; Termansen, M.; Zandersen, M.; Perez-Soba, M.; Scholefield, P.A.; Bidoglio, G. Mapping cultural ecosystem services: A framework to assess the potential for outdoor recreation across the EU. *Ecol. Indic.* **2014**, *45*, 371–385. [CrossRef]
23. Baró, F.; Palomo, I.; Zulian, G.; Vizcaino, P.; Haase, D.; Gómez-Baggethun, E. Mapping ecosystem service capacity, flow and demand for landscape and urban planning: A case study in the Barcelona metropolitan region. *Land Use Policy* **2016**, *57*, 405–417. [CrossRef]
24. Arnaiz-Schmitz, C.; Herrero-Jáuregui, C.; Schmitz, M.F. Recreational and nature-based tourism as a cultural ecosystem service: Assessment and mapping in a rural-urban gradient of central Spain. *Land* **2021**, *10*, 343. [CrossRef]
25. Wang, Z.; Jian, Y.; Huang, Z.; Qureshi, S.; Cheng, K.; Bai, Z.; Zhang, Q. Transforming research on recreational ecosystem services into applications and governance. *Land* **2023**, *12*, 509. [CrossRef]
26. Han, Y.; Wang, Y.; Yu, H.; Luo, W.; Wang, K.; Sui, C. Spatial synergy between tourism resources and tourism service facilities in mountainous counties: A case study of Qimen, Huangshan, China. *Land* **2024**, *13*, 999. [CrossRef]
27. Ministry of Culture and Tourism of the People's Republic of China. 2025 Domestic Tourism Data. Available online: https://zwgk.mct.gov.cn/zfxxgkml/tjxx/202601/t20260126_964367.html (accessed on 21 September 2026). (In Chinese)
28. National Bureau of Statistics of China. Statistical Communiqué of the People's Republic of China on the 2025 National Economic and Social Development. Available online: https://www.stats.gov.cn/sj/zxfb/202602/t20260228_1962662.html (accessed on 21 September 2026). (In Chinese)
29. State Council of the People's Republic of China. The 14th Five-Year Plan for Tourism Development. Available online: https://app.www.gov.cn/govdata/gov/202201/20/480985/article.html (accessed on 21 September 2026). (In Chinese)
30. National Development and Reform Commission. The State Council Approves the Territorial Spatial Plan for the Yangtze River Economic Belt-Yangtze River Basin (2021–2035). Available online: https://cjjjd.ndrc.gov.cn/zxdt/202402/t20240219_1364089.htm (accessed on 21 September 2026). (In Chinese)

31. Kádár, B.; Gede, M. Tourism flows in large-scale destination systems. *Ann. Tour. Res.* **2021**, *87*, 103113. [CrossRef]
32. Shih, H.-Y. Network characteristics of drive tourism destinations: An application of network analysis in tourism. *Tour. Manag.* **2006**, *27*, 1029–1039. [CrossRef]
33. Baggio, R.; Scott, N.; Cooper, C. Network science: A review focused on tourism. *Ann. Tour. Res.* **2010**, *37*, 802–827. [CrossRef]
34. Gao, Z.; Zeng, H.; Zhang, X.; Wu, H.; Zhang, R.; Sun, Y.; Du, Q.; Zhao, Z.; Li, Z.; Zhao, F.; et al. Exploring tourist spatiotemporal behavior differences and tourism infrastructure supply-demand pattern fusing social media and nighttime light remote sensing data. *Int. J. Digit. Earth* **2024**, *17*, 2310723. [CrossRef]
35. Sun, X.; Liu, H.; Liao, C.; Nong, H.; Yang, P. Understanding recreational ecosystem service supply-demand mismatch and social groups' preferences: Implications for urban-rural planning. *Landsc. Urban Plan.* **2024**, *241*, 104903. [CrossRef]
36. Liu, T.; Yu, L.; Liu, J.; Xu, Z.; Chen, X.; Wu, H.; Zheng, S.; Zhao, Q.; Gong, P. Unveiling interprovincial geographic patterns of 5A-level tourism cultural ecosystem service flows and tourist preferences in China's metacoupled systems. *Appl. Geogr.* **2024**, *172*, 103432. [CrossRef]
37. Wu, P.; Zhu, X.; Feng, X.; Liu, H.; Dong, J. Network characteristics of inter-city tourist flows in the Yangtze River Delta of China: Case study of the May Day Holiday based on Tencent migration big data. *Environ. Dev. Sustain.* **2025**, *27*, 10041–10058. [CrossRef]
38. Zhang, Z.; Wang, F.; Deng, L. Identifying node-corridor-network of tourist flow and influencing factors using GPS big data: A case study in Gansu and Qinghai provinces, China. *Int. J. Appl. Earth Obs. Geoinf.* **2024**, *135*, 104271. [CrossRef]
39. Confente, I.; Mazzoli, V.; Camatti, N.; Bertocchi, D. Integrating tourists' walk and talk: A methodological approach for tracking and analysing tourists' real behaviours for more sustainable destinations. *J. Sustain. Tour.* **2024**, *32*, 2323–2343. [CrossRef]
40. Ministry of Culture and Tourism of the People's Republic of China. Sichuan Advances the Development of the Sichuan Section of the Yangtze River International Golden Tourism Belt. Available online: https://www.mct.gov.cn/whzx/qgwhxxlb/sc/202206/t20220607_933382.htm (accessed on 21 September 2026). (In Chinese)
41. Silverman, B.W. *Density Estimation for Statistics and Data Analysis*; Chapman and Hall: London, UK, 1986.
42. Zhang, T.; Wang, Y.; Wang, Y.; Zhang, S.; Yu, H. Spatial structure and development of tourism resources based on point pattern analysis: A case study in Hainan Island, China. *J. Resour. Ecol.* **2022**, *13*, 1058–1073. [CrossRef]
43. Jenks, G.F. The data model concept in statistical mapping. *Int. Yearb. Cartogr.* **1967**, *7*, 186–190.
44. Newman, M.E.J. The structure and function of complex networks. *SIAM Rev.* **2003**, *45*, 167–256. [CrossRef]
45. Barrat, A.; Barthélemy, M.; Pastor-Satorras, R.; Vespignani, A. The architecture of complex weighted networks. *Proc. Natl. Acad. Sci. USA* **2004**, *101*, 3747–3752. [CrossRef]
46. Opsahl, T.; Agneessens, F.; Skvoretz, J. Node centrality in weighted networks: Generalizing degree and shortest paths. *Soc. Netw.* **2010**, *32*, 245–251. [CrossRef]
47. Wang, L.; Wu, X.; He, Y. Nanjing's intracity tourism flow network using cellular signaling data: A comparative analysis of residents and non-local tourists. *ISPRS Int. J. Geo-Inf.* **2021**, *10*, 674. [CrossRef]
48. Zhang, J.; He, C.; Huang, Q.; Li, J.; Qi, T. Evaluating the supply and demand of cultural ecosystem services in the Tibetan Plateau of China. *Landsc. Ecol.* **2022**, *37*, 2131–2148. [CrossRef]
49. Guo, Y.; Fu, B.; Wang, Y.; Xu, P.; Liu, Q. Identifying spatial mismatches between the supply and demand of recreation services for sustainable urban river management: A case study of Jinjiang River in Chengdu, China. *Sustain. Cities Soc.* **2022**, *77*, 103547. [CrossRef]
50. Ghasemi, M.; Charrahy, Z.; González-García, A. Mapping cultural ecosystem services provision: An integrated model of recreation and ecotourism opportunities. *Land Use Policy* **2023**, *131*, 106732. [CrossRef]
51. Li, C.; Liang, Q.; Lin, B.; Zhai, J. Landscape management and planning as a spatial organization method connecting CES supply-demand assessment and sustainable tourism development. *J. Outdoor Recreat. Tour.* **2023**, *44*, 100705. [CrossRef]
52. Dang, H.; Li, J. Supply-demand relationship and spatial flow of urban cultural ecosystem services: The case of Shenzhen, China. *J. Clean. Prod.* **2023**, *423*, 138765. [CrossRef]
53. Gao, J.; Peng, P.; Lu, F.; Claramunt, C. A multi-scale comparison of tourism attraction networks across China. *Tour. Manag.* **2022**, *90*, 104489. [CrossRef]
54. Qin, X.; Li, X.; Chen, W.; Tan, H.; Luo, L.; Xu, X. Tourists' digital footprint: The spatial patterns and development models of rural tourism flows network in Guilin, China. *Asia Pac. J. Tour. Res.* **2022**, *27*, 1336–1354. [CrossRef]
55. Chen, X.; Huang, Y.; Chen, Y. Spatial pattern evolution and influencing factors of tourism flow in the Chengdu-Chongqing Economic Circle in China. *ISPRS Int. J. Geo-Inf.* **2023**, *12*, 121. [CrossRef]

Disclaimer/Publisher's Note: The statements, opinions and data contained in all publications are solely those of the individual author(s) and contributor(s) and not of MDPI and/or the editor(s). MDPI and/or the editor(s) disclaim responsibility for any injury to people or property resulting from any ideas, methods, instructions or products referred to in the content.